Composites Communications 24 (2021) 100617

Contents lists available at ScienceDirect

Composites Communications

journal homepage: www.elsevier.com/locate/coco

A mini review on thermally conductive polymers and polymer-based composites

Yanfei Xu [a], Xiaojia Wang [b], Qing Hao [c,*]

[a] Department of Mechanical and Industrial Engineering, University of Massachusetts Amherst, 160 Governors Drive, Amherst, MA, 01003, USA
[b] Department of Mechanical Engineering, University of Minnesota, 111 Church St. SE, Minneapolis, MN, 55455, USA
[c] Aerospace & Mechanical Engineering, University of Arizona, 1130 N Mountain Ave, Tucson, AZ, 85721, USA

ARTICLE INFO

Keywords:
Polymer
Strain
Filler
Thermal conductivity

ABSTRACT

The continuous trend of miniaturization leads to unprecedented power densities within electronic devices, which also becomes the bottleneck of the device performance. Effective cooling of electronic devices is critical and polymer-based materials may play an important role in this important direction, with advantages such as low cost, corrosion resistance, light weight, and flexibility. For thermal management applications, the intrinsically low thermal conductivities of amorphous polymers can be dramatically enhanced with strain-induced crystallization and ultra-high-conductivity fillers. In this mini review, some advancements in this field are summarized and discussed, followed by a prospective on future directions.

1. Introduction

The continuously increasing power densities within electronic devices have created challenges for their thermal management and triggered active research over the years [1–6]. A new focus is on power electronic devices that are widely used for hybrid/electric vehicles, aircraft, satellites, smartphones, electric grids, and radar systems [7]. Despite numerous studies on coolers integrated with a chip [7,8], the overall heat rejection from a chip to the environment should also be addressed. Fig. 1 shows the typical scheme of electronics package, in which heat generated within a chip is eventually transferred to a heat sink or cold plate. The bottleneck for heat dissipation can be from interfacial thermal resistances within the chip [9,10] and between different components of the setup.

In applications, polymer-based materials can play an important role in reducing the above-mentioned thermal contact resistance within the packaging. For thermal management of electronic devices, one research focus is to minimize the thermal contact resistance between the chip and the heat sink, e.g., a fin or a cold plate (Fig. 1a). For two typical adjoining surfaces, their microscopic roughness results in an actual contact area that is only 1–2% of the nominal surface area [11,12]. To better "bridge" the two surfaces thermally, various thermal interface materials (TIMs) have been developed to facilitate the heat transfer. TIMs are typically compliant greases, gels, metallic solders or foils, filled polymer matrices, carbon-based materials, or phase change materials (PCMs) that work to compensate for the roughness of the interfacing surfaces by filling in the non-contacting areas that would otherwise be occupied by poorly conducting air gaps (Fig. 1b) [4,6,13–16]. Here polymer-based TIMs have been widely used in many applications with their mechanically flexibility, small thermal expansion coefficients, easy processing, and low cost. The obtained thermal resistance per unit area with a TIM is given as $R_{TIM} = t/k_{TIM} + R_{C1} + R_{C2}$, in which t is the TIM layer thickness, k_{TIM} is the thermal conductivity of the TIM, R_{C1} and R_{C2} are the thermal contact resistances between the TIM and each surface per unit area. The intrinsically low thermal conductivity k of polymers, as 0.1–0.5 W/m·K at room temperature, can largely restrict the performance of TIMs. For polymer-based TIMs, the highest k_{TIM} is 14 W/m·K with 2 vol % graphene fillers in a commercial thermal grease with its initial $k \approx 5.8$ W/m·K [17], whereas k_{TIM} is less than 8 W/m·K in most cases. Typical industrial TIMs have R_{TIM} of 3–10 $\times$ 10^{-6} m^2 K/W [13]. Continuous efforts can be found for enhancing the k of polymers by adding various high-thermal-conductivity fillers. Such composite materials could be readily integrated with existing technologies for better heat dissipation in microelectronics packaging. This composite-based approach involves embedding fillers (good thermal conductors) into flexible host media to improve the overall thermal performance.

In the setup shown in Fig. 1a, a heat spreader on top of a chip can also help to spread out the heat and thus minimize the temperature rise

* Corresponding author.
E-mail address: qinghao@email.arizona.edu (Q. Hao).

https://doi.org/10.1016/j.coco.2020.100617
Received 15 November 2020; Received in revised form 23 December 2020; Accepted 27 December 2020
Available online 5 January 2021

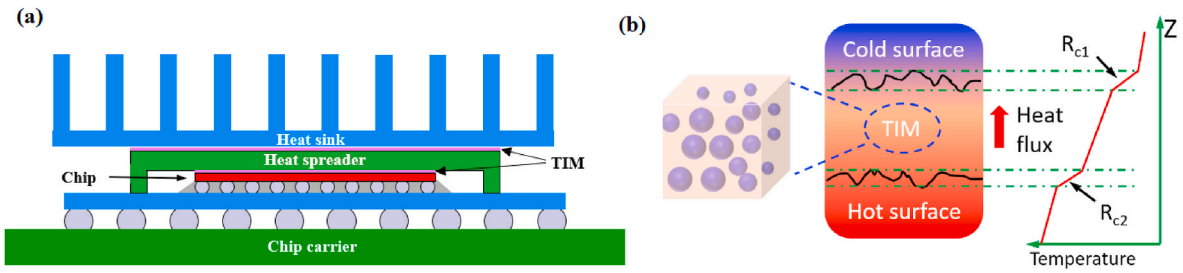

Fig. 1. (a) Schematic of a typical ball grid array electronics package with two TIM layers to improve the thermal transport between adjacent components. The major thermal resistances include the internal conduction thermal resistance within the chip, and the associated conduction/convection thermal resistance of the heat sink as a fin here. (b) Working principle of a TIM, where the airgap between two surfaces is filled with a TIM to reduce the interfacial temperature jump.

across the chip. Polymer-based thin films with an ultra-high thermal conductivity hold great promise for such applications. In addition, polymers can also be used for the usually metal-made heat sinks [18], as an extension from polymer-based heat exchangers developed at DuPont back in 1965 [19]. Despite the relatively low k of polymers with after adding fillers, polymer-based heat sinks have already become an alternative for metallic heat sinks for low heat flux applications, with advantages such as low cost, low weight, and good electrical insulation.

In this mini review, the recent advancements of polymers with enhanced thermal conductivities are summarized. The focus is on how to better align the random polymer chains with an applied strain and how to form a thermally conductive network with fillers such as nanocarbon materials.

2. Strain-induced chain alignment and crystallization within polymers

2.1. Current understanding of heat transfer in polymers

Polymers are generally regarded as thermal insulators [20–23]. Pervasive defects and structural disorders in polymers act as scattering sites for heat carriers, which lead to a low thermal conductivity on the order of 0.1 W/m·K [24,25]. For example, polymer chain entanglements, chain ends, crystal-amorphous interfaces, and voids hinder efficient thermal transport [21] (Fig. 2a). However, simulation studies have suggested that an extremely high thermal conductivity can be achieved in polymers [26,27]. Atomistic simulations have suggested that an individual crystalline polyethylene chain can have a very high—possibly divergent—thermal conductivity [27], in agreement with the non-ergodic characteristics of one-dimensional conductors discussed by Fermi et al. [28]. The fact that common polymers (e.g., polyethylene) are composed of backbones of covalent carbon-carbon bonds similar to those in diamond, one of the most thermally conductive materials (above 1000 W/m·K), encourages research in developing thermally conductive polymers with a diamond-like thermal conductivity (Fig. 2b) [29,30].

Over the past decades, considerable progress has been made in the development of thermally conductive polymers [21,23,32–34]. A record-high thermal conductivity for polymers has been measured in polyethylene nanofibers (~104 W/m·K), which is 300 times higher than that of bulk polyethylene (~0.35 W/m·K). Although exceptionally conductive, this measured thermal conductivity is lower than the numerical predictions for single-crystalline polyethylene (~160 W/m·K [35]). There is no precise mechanism that accounts for the deviation of experimental and theoretical values [35]. To date, a systematic theory of the thermal transport in bulk polymers is still lacking [32].

Further understanding of the thermal transport mechanisms in polymers is essential for designing and developing the next generation of thermally conductive polymers [20,23,36]. In particular, understanding the relationships between the thermal conductivity and polymer structures (chemical composition, chain alignment and crystallinity, chain morphology and topology) is essential for controlling thermal transport in polymers [1,20,23,29,36–42]. In this section, we will focus on how chain alignment and crystallinity influence the thermal conductivity of polymers. We will review how the thermal conductivity is enhanced by strain-induced polymer chain alignment and crystallization.

The thermal conductivity in polymers is morphology dependent [31,43]. An enhanced thermal conductivity along chain directions has been measured in aligned polymers [44–46]. During chain alignment processes, crystalline domains are orientated, and coiled and amorphous chains also become more orientated. After chain alignments, heat carriers can transport more efficiently along these straight chains, which results in an enhanced thermal conductivity in the aligned chain directions. In addition to semicrystalline polymers, a high thermal conductivity has also been measured in aligned amorphous polymers [47,48]. Detailed examples for a high thermal conductivity in aligned polymers will be discussed below.

The thermal conductivity in polymers is also crystallinity dependent [23,49–56]. In common polymers including semicrystalline polymers and amorphous polymers, amorphous domains hinder efficient thermal transport by disorder scatterings and lead to a low thermal conductivity. In semicrystalline polymers, from the amorphous domains to crystalline domains, the thermal conductivity of polyethylene has been predicted to increase from 0.3 W/m·K to 50 W/m·K by molecular dynamics (MD) simulations [41]. The low thermal conductivity in amorphous domains could root from conformational disorders that significantly interrupt heat carrier transport along chains [57]. Crystalline polymers usually have a higher thermal conductivity than amorphous ones [58]. Crystallization can increase the intrinsic order, which is likely responsible for a higher thermal conductivity in polymers such as polytrifluorochloroethylene [34] and polyethylene [59]. However, there are exceptions. For example, polypropylene is highly crystalline but has a low thermal conductivity [58]. The low thermal conductivity of polypropylene can be attributed to its low crystal density, and/or the possible heat carrier scatterings created by the vibrational mode of methyl side group, and/or the possible heat carrier scatterings at interfaces between crystallites and the amorphous domains [58]. Thus, the thermal conductivity of polymers is not solely controlled by crystallinity. There are other key structural factors influencing the thermal conductivity, which could be crystal structures, chain structures, monomer structures, chain conformations, chain morphologies and topologies, and among others [21,23,31–34,43].

2.2. Enhancing the thermal conductivity of polymers via strain engineering

To decrease structural disorders and increase chain alignments, uniaxial (or biaxial) mechanical stretching has been widely used for aligning polymer chains [60–62]. Meanwhile, strain-induced crystallization may occur through chain alignment, rotation, and perfection of internal order of paracrystalline structures that originally present in amorphous chains [31,63–67] (Fig. 3). In stretched polymers, more

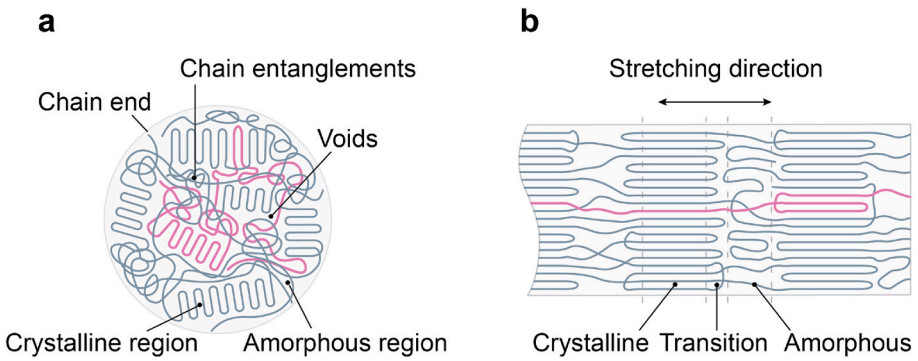

Fig. 2. (a) Illustration of polymer structures with amorphous and crystalline regions. In the amorphous regions, there are chain entanglements, chain voids and ends limit efficient heat transfer in polymers. (b) Illustration of polymer structures with better chain alignment and higher crystallinity [31], which are expected to provide efficient thermal transport pathways.

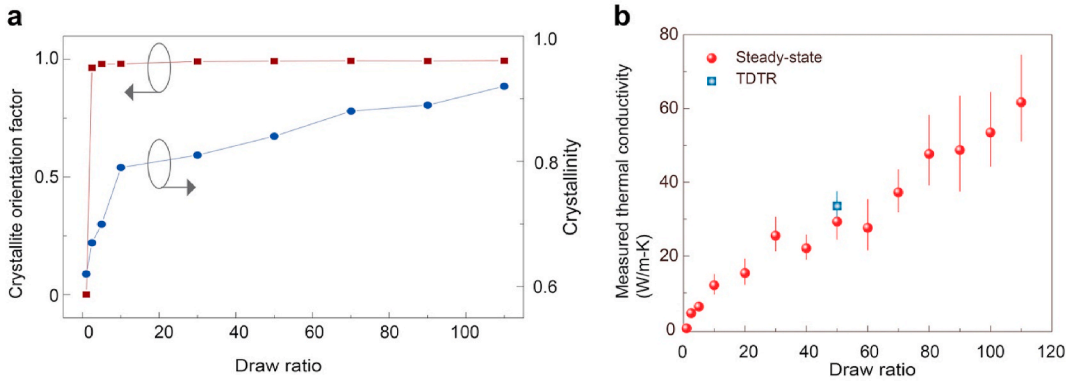

Fig. 3. (a) First-order orientation parameter and the effective crystallinity in stretched polyethylene films under different draw ratios. (b) Measured total thermal conductivity in stretched polyethylene as a function of the draw ratio. The red spheres were obtained from the steady-state experiments. A thermal conductivity of 62 W/m·K was measured from the × 110 films. The blue square denotes the average of 20 transient thermoreflectance measurements at 3 and 6 MHz modulation. The steady-state error bars take into account the uncertainties in the measurement of the sample geometry, the uncertainty in the estimation of the radiation contribution and the uncertainty in the thermal shunting measurement [31]. (For interpretation of the references to colour in this figure legend, the reader is referred to the Web version of this article.)

covalent bonds in polymer backbones are expected to be oriented along the stretching direction than other directions (Fig. 3a). Aligned backbones are expected to provide efficient thermal pathways. An enhanced thermal conductivity has been measured for stretched polymers [23,31,38–40,51–53,68–74]. For example, a room-temperature thermal conductivity of ~20 W/m.K has been reported for stretched polyethylene mirofibers and poly(p-phenylene benzobisoxazole) microfibers, which have high tensile moduli and are commercially available [53]. In addition, the one-dimensional polyethylene nanofibers have a high thermal conductivity ~104 W/m·K along the stretched chain direction [52], which exceeds that of ceramics and many metals. The high thermal conductivity ~104 W/m·K of polyethylene is attributed to the restructuring of the polyethylene chains by stretching, which improves the fiber quality toward an 'ideal' single crystalline fiber. These polyethylene nanofibers with 'perfect' single crystalline structures are created from a polyethylene gel prepared by dissolving ultrahigh-molecular-weight polyethylene powder in decalin at 1451°C. The solution is then quenched in water to form a gel. Subsequently, a small sample of wet gel is heated to 120°C on a heating stage and an individual suspended fiber is drawn from the heated gel using either a sharp tungsten tip or a tip-less atomic force microscope cantilever (diameter, ~100 nm). The overall draw ratio for drawn polyethylene fibers has been estimated to be between 60 and 800 [52]. Here the draw ratio is the final length divided by the initial length [52]. The polyethylene nanofibers have a thermal conductivity ~104 W/m·K, when the draw ratio is 410 [52]. Through the Couette-flow extrusion and roll-to-roll stretching processes, polyethylene films are developed with an emphasis on minimally entangling and maximally aligning the polyethylene chains [31]. Such stretched polyethylene films with disentangled and aligned chains show a high thermal conductivity ~62 W/m·K along the stretching direction (draw ratio 110) [31]. The thermal conductivity and crystallinity in these polyethylene films increase with increasing draw ratios (Fig. 3a and b). Disentangled polyethylene can also be processed in the solid states through compaction followed by uniaxially stretching [69]. The obtained stretched polyethylene films have a high thermal conductivity ~61.8 W/m·K (draw ratio 240) along the stretching direction [69]. An enhanced thermal conductivity (~9.3 W/m·K) has been measured in stretched semicrystalline polyethylene films (draw ratio 7.5), and quasiballistic heat transport has been experimentally probed in these stretched polyethylene films, and ballistic phonons with mean free paths up to 200 nm has been experimentally probed [75]. The polymer films with higher draw ratios have better chain alignments and higher crystallinity, which results in a higher thermal conductivity [31,69,75]. Zylon fibers show a high thermal conductivity ~20 W/m·K along the fiber direction [53]. PMMA shows a thermal conductivity ~0.29 W/m·K (stretching degree two) along the stretching direction, which is 1.7 times higher than that of unstretched one [72]. Attention should also be paid to the anisotropy of the thermal conductivity of stretched polymers [31,52,69,76,77]. The high thermal conductivity is only measured in the stretched chain direction, the thermal conductivity across the chain direction is still on the order of 0.1 W/m·K [77]. This is because, unlike strong carbon-carbon covalent bonds (~346 kJ/mol) in polymer

backbones, common intermolecular interactions between polymer backbones are weak Van der Waals forces (~0.4 kJ/mol to 4 kJ/mol) [23,29,78]. Synthesizing bulk polymer single crystal is an effective way to decrease disorders and increase the thermal conductivity, but it remains very challenging [54,79].

In contrast to above uniaxially stretched polymer fibers and films, the biaxially stretched polyethylene films also show a high thermal conductivity of 18 W/m·K in the in-plane direction, which is comparable to stainless steel [69,80] (Table 1). The high thermal conductivity of the biaxial drawn polyethylene films, with a thickness of 30 μm, can be attributed to the extended chain orientation in the biaxial direction, thus facilitating the efficient thermal transport [69].

In addition to mechanical stretching methods for making strain-induced chain alignments, polymer chain orientations can be induced by the extensional flow of electrospinning [81,82]. During electrospinning, a strong electrostatic field forces a liquid jet from a droplet of dissolved polymer chains, and a continuous nanofiber is formed as the solvent evaporates in flight [83–86]. The strong elongational flow in this jet can result in fibers with chain orientations, which are expected to have a significantly enhanced thermal conductivity along the fiber direction [83–86]. In addition to chain alignments, there could be reduction in defects and voids in the electrospun polymer fibers [86]. The aligned polymer chains by electrospun methods are expected to provide efficient thermal transport pathways [87]. For example, polyethylene nanofibers produced at a 45 kV electrospinning voltage and a 150 mm needle-collector distance could have a thermal conductivity of up to 9.3 W/m·K, over 20 times higher than the typical bulk value [83]. Electrospun Nylon-11 fibers show a thermal conductivity ~1.6 W/m·K, which is ~10 times higher than that of the unstretched one [84]. Electrospun polyethylene oxide has a thermal conductivity of ~29 W/m·K [85]. Compared with the ~0.5 W/m·K thermal conductivity in electrospun polyvinyl chloride fibers, polyvinylidene fluoride fibers show a higher thermal conductivity of ~0.9 W/m·K [86]. This is because the vibrational energy can propagate more efficient along polyvinylidene fluoride chains, when the side groups are lighter and more symmetric [86]. Electrospun polystyrene nanowires have a thermal conductivity of ~14.4 W/m·K, which is a significant increase from typical bulk values [87]. This is because the vibrational energy can propagate more efficient along the aligned polystyrene chains than that of typical coiled polystyrene chains.

2.3. Knowledge gap between theoretical and experimental studies

Although an ultrahigh thermal conductivity has been measured in above stretched polymers, for example, stretched polyethylene nanofibers and films [31,52], the measured values are still much lower than the numerical predictions for 1D crystalline polyethylene fibers (~350 W/m·K or possibly divergent) [27] and bulk single-crystalline polyethylene (~160 W/m·K) [27,35,42]. To date, there is no precise mechanism that accounts for the deviation of experimental and theoretical values. The interplay between thermal transport properties and polymer structures remains not fully understood. Future design and development of the next generation of heat conducting polymers with a diamond-like thermal conductivity require in-depth understanding of thermal transport mechanisms at multiscale levels ranging from the atomic level and the nanoscale level to the microscale level and the macroscale level.

Table 1
High thermal conductivities of uniaxially and biaxially stretched polymers [31,52,69].

Sample	Total draw ratio	Thermal conductivity (W/m·K)
Polyethylene nanofiber [52]	400	104/along fiber direction uniaxial stretched sample
Polyethylene film [31]	110	62/along stretching direction uniaxial stretched sample
Polyethylene film [69]	240	61.8/along stretching direction uniaxial stretched sample
Polyethylene film [69]	3.8 × 3.2 for biaxial directions	18.4/in-plane direction biaxial stretched sample

3. Polymer-based composites with fillers

3.1. Overview for thermal conductivity enhancement with fillers

Polymeric nanocomposite-based TIM materials by loading a matrix with high thermal conductivity micro- or nano-fillers is a common approach that can be readily accepted for practical use. A variety of micro- and nano-fillers have been investigated in literature, including alumina [88], silica [88,89], boron nitride [88,90,91], aluminum nitride [92], silicon carbide [93], graphite [88], diamond [88,90], graphene [91,94], carbon nanotubes [93,95], carbon fibers [89], and few-layer materials [94,96]. A brief summary of employed fillers and their thermal conductivities (k_f) can be found elsewhere [4,97]. More advanced studies can also be found for fully carbon-based fillers made of functionalized multi-walled carbon nanotubes and reduced graphene oxide [98]. Literature studies have demonstrated significant increase in the thermal conductivity for composites compared with that of the pure host material. However, due to the low thermal conductivity of the host media (e.g., ~0.2 W/m·K for polymers), the gain in the effective thermal conductivity of composites is rather moderate, often less than 10 W/m·K [99]. As a few exceptions, a thermal conductivity of 32.5 W/m·K was reported for 78.5% (volumetric) boron nitride-loaded polybenzoxazine [100] and a thermal conductivity of 14 W/m·K was reported for a commercial thermal grease loaded with graphene fillers [17].

3.2. Effective medium formula and the importance of R_K

The effective thermal conductivity k_{eff} for polymers with dispersed fillers depends on the thermal conductivity k_h of the polymer host, the thermal conductivity k_f of the filler or inclusion, the volumetric fraction ϕ of fillers, and the interfacial thermal resistance R_K between the filler and the polymer host [13]. Some insights for the future development of TIMs can be obtained from the thermal modeling of a nanocomposite. Effective medium approximation (EMA) models are generally used to predict the thermal conductivity of various composites. EMA models usually assume dispersion of isolated fillers in a continuous matrix and can take into account the interfacial thermal resistance R_K (or the inverse of resistance, interfacial thermal conductance) between the filler and the host [101–104]. For an isotropic polymer host embedded with spherical particles, the effective k_{eff} for such a particle-in-a-host geometry is given under the EMA [105–107]:

$$\frac{k_{eff}}{k_h}=\frac{k_f(1+2\alpha)+2k_h+2\phi\left[k_f(1-\alpha)-k_h\right]}{k_f(1+2\alpha)+2k_h-\phi\left[k_f(1-\alpha)-k_h\right]}. \quad (1)$$

Here the dimensionless α is defined as $2R_Kk_h/d$, where d is the particle diameter and R_K is the thermal interface resistance between the particle and the polymer. Equation (1) has been widely used for polymer-based TIMs, particle-fluid mixtures [108], and nanocomposites with classical phonon size effects associated with nanostructures [109,110]. For composites with fillers in contact with each other, the EMA model can be further modified to incorporate the contact resistance between fillers [111–113].

When $k_f \gg k_h$ is given for fillers with ultra-high thermal conductivities, Eq. (1) can be approximated as [106].

$$\frac{k_{eff}}{k_h}=\frac{1+2\alpha+2\phi(1-\alpha)}{1+2\alpha-\phi(1-\alpha)}. \quad (2)$$

Equation (2) can be valid for polymers filled with particles possessing a significantly higher thermal conductivity than the polymer host.

Two extreme cases related to R_K should be pointed out for Eq. (1). In

one case, $R_K = \alpha = 0$ is considered, assuming perfect thermal contacts between particle fillers and the host. Equation (1) then degrades into the well-known Maxwell formulation [114]:

$$\frac{k_{eff}}{k_h} = \frac{k_f + 2k_h + 2\phi\left[k_f - k_h\right]}{k_f + 2k_h - \phi\left[k_f - k_h\right]}. \tag{3}$$

Another extreme case occurs when $\alpha \to \infty$ for small d and large R_K. In this situation, the nanoparticles function as nanopores and Eq. (1) becomes the Eucken's formulation for a bulk material with cubically aligned spherical pores [115]:

$$\frac{k_{eff}}{k_h} = \frac{1-\phi}{1+\phi/2}, \tag{4}$$

which yields the minimum k_{eff} value for a given ϕ. The Eucken's formulation is widely used for the thermal conductivity predictions of porous bulk materials [116,117]. However, a high α should be avoided for TIMs or heat spreaders. As one example, the thermal conductivity of a ZnS host can be even lowered by the addition of sub-micron size particles of diamond though adding large diamond particles can still benefit k_{eff} [118]. In practice, a relatively large α indicates R_K is the bottleneck for thermal transport so that further increasing k_f may not largely benefit k_{eff}.

Following the EMA formula, several studies have reported that the improvement of the k_{eff} value may be limited by the high thermal resistance R_K at the filler-host interfaces [119,120]. Such a high R_K is attributed to the weakly bonded interfaces (e.g., van der Waals interaction) typically formed between the fillers and the host medium that are dissimilar from each other. The bonding studies can also be found out in the mechanical studies of these composites [121]. In some papers, this interfacial resistance R_K is modelled as the acoustic mismatch between the polymer and the filler, and the incomplete wetting on the interface by the polymer. In the analysis by Prasher et al. for various polymer-based TIMs [13,122], the acoustic mismatch only accounts for $R_K \sim 10^{-8}$ m^2 K/W so that the extracted $R_K \approx 5 \times 10^{-6}$ m^2 K/W is mainly attributed to the incomplete wetting. Other factors, such as molecule line-up at the interfaces, are also proposed [123]. On the other side, direct measurements [124] and simulations to fit the experimental data [125,126] show an interfacial R_K of 1×10^{-9} to 1.5×10^{-7}m^2 K/W between nanocarbon materials and various host materials. Depending on the fillers and the preparation methods, large divergence in R_K is anticipated. The part of R_K due to acoustic mismatch, as predicted by MD simulations [127] and less accurate analytical models [128,129], can be viewed as the lower bound in thermal modeling. In practice, the improvement of the thermal performance of composites is rather modest by merely increasing the filler loading rate, approaching or exceeding the percolation threshold. Doing so will not only significantly increase the material cost but may also change other important properties of the composites such as mechanical, electrical, and optical properties. Thus, the enhancement of thermal performance of composite-based TIMs shall also consider tailoring the thermal properties of the polymer host and engineering the thermal interface between the fillers and the host.

3.3. Effective medium formula for high- ϕ cases and non-spherical fillers

In principle, Eq. (1) is only suitable for a low volume fraction ϕ of discrete inclusions completely dispersed in a matrix. Typically, ϕ<0.4 is required [4]. For a higher ϕ, the self-consistent EMA is more suitable. For an isotropic particle-in-a-host system, k_{eff} can be solved from [130]

$$(1-\phi)\frac{k_h - k_{eff}}{k_h + 2k_{eff}} + \phi\frac{k_f - k_{eff}\left(1+\alpha k_f/k_h\right)}{k_f + 2k_{eff}\left(1+\alpha k_f/k_h\right)} = 0. \tag{5}$$

At the limit of $\alpha = 0$, Eq. (5) simply degrades into the self-consistent Bruggeman EMA formulation [131]. In addition, the Bruggeman asymmetric model is also available for a high ϕ [118]:

$$(1-\phi)^3 = \left(\frac{k_h}{k_{eff}}\right)^{(1+2\alpha)/(1-\alpha)} \left[\frac{k_{eff} - k_f(1-\alpha)}{k_h - k_f(1-\alpha)}\right]^{3/(1-\alpha)}, \tag{6}$$

with its simplified form at the limit $\alpha = 0$ or $k_f \gg k_h$. More comparison between the Bruggeman asymmetric models and experimental data can be found in Prasher et al. [13,122].

Other than particle-like fillers considered in Eqs. (1)–(6), EMA formula have been developed to compute the enhanced k_{eff} for a host material with dispersed fibers (nanotubes), laminated flat plates, and ellipsoidal particles [105,130,132,133]. Among employed fillers, nanocarbon materials have the highest thermal conductivities, e.g., graphene with in-plane k_f of 2000–4000 W/m·K at room temperature for fully suspended samples [30,134,135]. However, the ultrasmall structure size leads to a higher α. In this case, R_K becomes critical to the thermal transport. It has also been acknowledged that the alignment of fillers with a high aspect ratio can be critical to the k_{eff} enhancement. Compared with TIMs with randomly oriented nanostructures, aligned carbon nanotubes [136–139] or graphene films [140] within a polymer host can achieve a much higher k_{eff} along the aligned direction.

3.4. Thermal percolation

A significantly increased k_{eff} can be obtained when an ideal thermal conducting network can be formed among embedded nanostructures, known as "thermal percolation" [141–144] (Fig. 4 as the case with single fillers). The critical filler fraction to induce the network formation is called the percolation threshold. Without percolations, the interfacial R_K between the nanostructures and the polymer host may strongly suppress the thermal transport. When a 3D network is formed, heat can be largely transferred through the network and the thermal resistance at the junctions between joined fillers becomes critical. It should be pointed out that the thermal conductivity increase associate with thermal percolation is not as remarkable as the electrical conductivity gain with the electrical percolation. The threshold ϕ for the thermal and electrical percolation may also diverge [144]. One argument is that the thermal conductivity contrast between the polymer and the fillers is orders of magnitude lower than the electrical conductivity contrast between the electrically insulated polymer and high-electrical-conductivity fillers like nanocarbon [144]. In modeling, $k_{eff} = \phi k_f/3$ is proposed for a composite with percolation [145], which significantly overpredicts the k_{eff} observed in polymers filled with carbon nanotubes. This divergence can be attributed to the actual orientation of carbon nanotubes and the interfacial thermal resistance between the carbon nanotubes and the polymer, and at the junctions between carbon nanotubes. In the study by Kargar et al. [144], the Lewis-Nielsen model [146,147] is found to be accurate for the data analysis

$$\frac{k_{eff}}{k_h} = \frac{1 + AB\phi}{1 - B\Psi\phi}, \tag{7}$$

with the constants A, B, and Ψ given for typical two-phase systems [147].

In numerous studies, hybrid fillers of 0D to 2D structures are also investigated to fill the voids and form a hybrid network consisting of different fillers [148–155] or cross-linked double networks [156,157], both with synergetic enhancement of the k_{eff}. More detailed reviews on the use of percolations to improve polymer-based TIMs are available [6,123,129]. In addition, 3D graphene or carbon foams [158–160] or expanded graphite [161–166] can also be used as fillers to avoid the possible aggregation of typical fillers. Table 2 summarizes representative TIMs for their thermal conductivities.

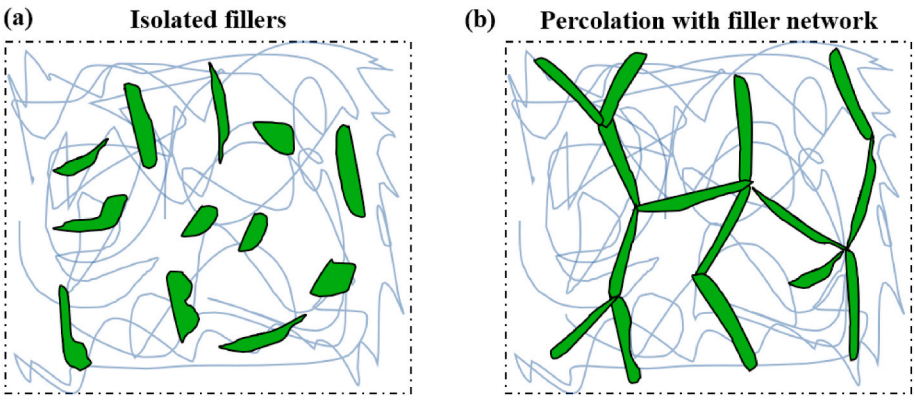

Fig. 4. Nanostructure-embedded polymer host (a) without and (b) with a thermally conductive network formed between nanostructures. The random blue curves in both figures are polymer chains. (For interpretation of the references to colour in this figure legend, the reader is referred to the Web version of this article.)

Table 2
Summary of representative TIMs with various fillers in polymer hosts.

Filler	Matrix	Filler Prep. Method	Composite Prep. Method	Filler % (Percolation)	*k* (W/m·K)	Years
v**Graphite nanoplatelet**	Epoxy	Expanded and sonicated	High shear mixing	≈34 wt% (NA)	6.44	**2007** [167]
Graphene nanoplatelet + CNT	Epoxy	Intercalation + exfoliation (GNP); electric arc (SWCNT)	shear mixing + sonication	7.5 wt% + 2.5 wt%	1.75	**2008** [152]
Functionalized exfoliated graphite	Epoxy	Silane functionalized	High shear mixing	20 wt% (NA)	5.8	**2008** [168]
Graphene + CNT	Epoxy	Methacrylate functionalized	High shear mixing	1 wt% (NA)	0.32	**2011** [149]
Graphene nanosheets	Epoxy	Pyrene derivatives functionalized	High shear mixing	4 wt% (NA)	1.91	**2011** [169]
Graphene + Multilayer graphene	Epoxy	Sodium cholate functionalized	High shear mixing	≈15 wt% (No)	5.1	**2012** [170]
Graphene nanoplatelet + CNT	Epoxy	Thermal exfoliation (GNP); MWCNT	Rotational mixing	20 vol% + 20 vol%	6.31	**2012** [157]
Graphene + CNT	Epoxy	GNP, multiwalled carbon nanotube	High shear mixing	50 wt% (Yes)	7.3	**2012** [157]
Graphene + Multilayer graphene	Epoxy	liquid-phase-exfoliation	Ultrasonication + centrifugation	10 vol% (No)	5.1	**2012** [17]
Functionalized graphene flakes	Epoxy	Pyrene derivatives functionalized	High shear mixing	10 wt% (NA)	1.53	**2013** [171]
Graphene nanoflake	Polytertafluoro-ethylene	-	Hot-pressed thermoplastic molding	≈24 wt% (NA)	10	**2015** [172]
Graphene nanoplatelet	Epoxy	Silane functionalized	Centrifugal mixing	15 vol% (Yes)	12.4	**2015** [173]
Ultrathin graphite foam + CNT	Erithrytol	Chemical vapor deposition	Melted into UGF	15.8 vol% (Yes)	4.09	**2015** [174]
Ag Flake + CNT	Epoxy	Ag-nanoparticle-functionalized CNT	High shear mixing	35.8 vol% Ag + 2.3 vol% CNT (Yes)	160	**2016** [175]
Graphene nanoplatelet	Polycarbonate	-	Melt-mixing	20 wt% (NA)	7.3	**2016** [176]
Multilayer graphene	Epoxy	Expanded and sonicated	High shear mixing	5.7 wt% (No)	1.5	**2016** [177]
Expanded graphite	Epoxy	Expanded via inductively couple plasma	Ultrasonic mixing	20 wt% (NA)	11	**2017** [178]
Graphene + Few-layer graphene flakes	Epoxy	-	High-shear speed mixing + stirring	45 vol% (Yes)	11	**2018** [124]
Graphene nanoplatelet	Carbon fiber reinforced polymer	-	Powder mixing	20 wt% (Yes)	13.70	**2018** [179]
Graphene nanoplatelet	Epoxy	-	High shear mixing	44 wt% (NA)	8.7	**2019** [180]
Graphene oxide	Epoxy	-	High shear mixing	6 wt% (Yes)	1.54	**2019** [181]

3.5. Fundamental studies on R_K and pressure influence

As discussed earlier, the bottleneck for heat transfer in TIMs using ultrafine fillers can be the R_K values at the filler-polymer interfaces. Accurate determination of the thermal interface between dissimilar materials is a challenge in the thermal community due to the lack of measurement sensitivity of direct experimental characterization. The transient absorption (TA) method, based on the ultrafast laser pump and probe technique, can probe thermal transport from fillers to the host medium with nanometer resolution. There are literature studies reporting high-sensitivity measurements of the interfacial thermal conductance between nanoparticles suspended in a liquid environment

[182–184]. This method can be extended to solid composite systems provided the host materials being transparent to the laser wavelength (typically ~780 nm) and the filler materials having decent optical absorption. Along this line, the first measurement by Cahill and Keblinski suggests R_K~8.3×10^{-8} m^2 K/W across the interface between a surfactant-coated single-wall carbon nanotube and its surrounding water [145], which is comparable to interfacial R_K in some polycrystals or composites [130,185,186].

Keeping the important of R_K in mind, tremendous efforts have been dedicated to improving the thermal contact between a nano-filler and the polymer host. For example, the thermal contact between 2D fillers and a polymer can be improved with surface coating [187,188], hydrogen-bonded interfaces [189] and functionalized self-assembled monolayers [126]. Based on MD simulations, Zhang and Liu have demonstrated that poly(vinyl alcohol) (PVA) monolayers with hierarchically arranged hydrogen bonds drastically enhance the interfacial thermal conductance by a factor of 6.22 across the interface between graphene and PMMA [189]. Their simulations also suggest that polyethylene (PE) self-assembled monolayer functionalized graphene surfaces can drastically improve the interfacial thermal conduction between graphene and the PMMA matrix [126]. However, these simulations have not been validated experimentally and can be costly in manufacturing processes. In addition, surface functionalization may sometimes deteriorate the interface thermal transport, according to MD simulations on graphene@polyamide-6.6 nanocomposites with surface-grafted chains [190]. In practice, surface coating with MgO [187] or Ag nanoparticles [188] may be more feasible and an enhanced k_{eff} is observed experimentally. In addition, Ag-nanoparticle-anchored reduced graphene oxide can also prevent the aggregation of graphene fillers in a polymer host [191]. For boron nitride fillers and a polyimide host, surface functionalization of these fillers can also reduce R_K and thus benefit k_{eff} of the composite [192]. Despite above successes, attention should be paid to the reduced k_f of the fillers due to coating or surface functionalization [123].

In applications, a pressure is often applied to improve the contact between the TIM layer and the opposite surfaces to be thermally bridged, leading to a reduced R_{TIM} value. In the total thermal resistance $R_{TIM} = t/k_{TIM} + R_{C1} + R_{C2}$ per unit area, both R_{C1} and R_{C2} can be reduced because of the increased contact area under an increased pressure P. For a given surface roughness σ, Prasher and Matyabus suggest that the dimensionless $R_C k_{TIM}/\sigma$ is inversely proportional to P [193]. When a high pressure is employed to ensure better thermal contacts, the k_{eff} of the TIM itself may change and should be calibrated. For long-term applications, the degradation of the TIMs should also be considered, particularly for harsh environments [4].

4. Summary and perspective

In summary, continuous progresses have been made on thermally conductive polymers and polymer-based composites. Rich physics exists in this research field, such as the interfacial thermal transport between a polymer and a nanostructure [129]. Challenges exist in reducing the polymer-filler R_K by modifying the surface of fillers, while suppressing the filler aggregation and minimizing the negative effect on the high thermal conductivities of the fillers [123]. For large-scale applications, the cost and manufacturing efficiency should also be considered. More effective methods to tailor the interfacial thermal transport are related to a broader field known as “interface engineering” for various device- and energy-related applications [1]. With accumulated experimental and simulation data, machine learning [194–196] may play an important role in guiding the materials design. The processing-structure-property relationship for polymer-based composites still needs to be better understood to further improve these composites for thermal, electrical, and mechanical properties. For the critical thermal percolation [6,123], existing knowledge is still very limited and a universal picture about the threshold of the thermal percolation is still lacking. Open questions remain on how to form a more effective heat conduction network with less thermal resistances between fillers. Further consideration may also focus on the mechanical properties and the modeling of k_{eff} above the percolation threshold. At the end, the wide applications of materials such as nanocarbon may also be hindered by the environmental and safety concerns. In 2020, carbon nanotubes have been added to the SIN (Substitute it Now!) list as a nanomaterial of very high concern [197]. In addition, more recent experiments using non-human primates show that blood exposure of graphene oxides may cause anaphylactic death [198]. Toxicological evaluation of nanocarbon for large-scale industrial production is critical now. Compared with other applications, above-mentioned composites have a very small amount of nanocarbon embedded in a polymer host, which minimizes the possible exposure of these materials. However, more attention should still be paid to the disposal of these composites as waste.

Along another line, the strain-induced crystallization of polymers can be further related to the “strain engineering” of materials [1,199,200]. A better understanding of the strain-related properties can also benefit applications such as flexible electronic devices. From the fundamental perspective, developing the next generation of heat-conducting polymers with diamond-like thermal conductivity, especially semi-crystalline and amorphous polymers, a deep understanding of the thermal transport mechanisms in polymers is required. From the application perspective, polymers with simultaneously high thermal conductivities and high melting temperatures are desirable for thermal management applications such as polymeric heat exchangers and heat spreaders.

Despite separated discussions for enhanced thermal conductivities with electrospinning and added fillers, the two approaches can be combined in some cases. For instance, boron nitride nanosheets/polyvinyl alcohol composite films prepared by electrospinning and subsequently hot pressing exhibit a parallel-direction k_{eff} of 18.630 W/m·K, which is an 3101.0% and 1437.1% increase compared to those of composite films synthesized by ball milling and directional freeze-drying, respectively [201]. Here electrospinning can help to better disperse and align the thermally conductive fillers. For various applications, the focus should also be on materials properties beyond the thermal conductivity, such as electrical insulating properties [202].

Declaration of competing interest

The authors declare that they have no known competing financial interests or personal relationships that could have appeared to influence the work reported in this paper.

Acknowledgements

Hao and Wang thank the support from National Science Foundation (grant number CBET-1803931). Yanfei Xu thanks the Faculty Startup Fund Support from University of Massachusetts Amherst.

References

[1] D.G. Cahill, P.V. Braun, G. Chen, D.R. Clarke, S. Fan, K.E. Goodson, P. Keblinski, W.P. King, G.D. Mahan, A. Majumdar, H.J. Maris, S.R. Phillpot, E. Pop, L. Shi, Nanoscale thermal transport. II. 2003–2012, Appl. Phys. Rev. 1 (1) (2014), 011305.

[2] D.G. Cahill, W.K. Ford, K.E. Goodson, G.D. Mahan, A. Majumdar, H.J. Maris, R. Merlin, S.R. Phillpot, Nanoscale thermal transport, J. Appl. Phys. 93 (2) (2003) 793–818.

[3] A.L. Moore, L. Shi, Emerging challenges and materials for thermal management of electronics, Mater. Today 17 (4) (2014) 163–174.

[4] Y. Zhou, S. Wu, Y. Long, P. Zhu, F. Wu, F. Liu, V. Murugadoss, W. Winchester, A. Nautiyal, Z. Wang, Recent advances in thermal interface materials, ES Materials & Manufacturing 7 (2020) 4–24.

[5] Y. Cui, M. Li, Y. Hu, Emerging interface materials for electronics thermal management: experiments, modeling, and new opportunities, J. Mater. Chem. C 8 (2020) 10568–10586. https://pubs.rsc.org/en/content/articlelanding/2020/t.
[6] F. Zhang, Y. Feng, W. Feng, Three-dimensional interconnected networks for thermally conductive polymer composites: design, preparation, properties, and mechanisms, Mater. Sci. Eng. R Rep. 142 (2020) 100580.
[7] Y. Won, J. Cho, D. Agonafer, M. Asheghi, K.E. Goodson, Fundamental cooling limits for high power density gallium nitride electronics, IEEE Trans. Compon. Packag. Manuf. Technol. 5 (6) (2015) 737–744.
[8] R. van Erp, R. Soleimanzadeh, L. Nela, G. Kampitsis, E. Matioli, Co-designing electronics with microfluidics for more sustainable cooling, Nature 585 (7824) (2020) 211–216.
[9] E. Pop, K.E. Goodson, Thermal Phenomena in Nanoscale Transistors, 2006.
[10] Q. Hao, H. Zhao, Y. Xiao, Q. Wang, X. Wang, Hybrid electrothermal simulation of a 3-D fin-shaped field-effect transistor based on GaN nanowires, IEEE Trans. Electron. Dev. 65 (3) (2018) 921–927.
[11] C.V. Madhusudana, Thermal Contact Conductance, Springer, 1995.
[12] M. Yovanovich, E. Marotta, Thermal spreading and contact resistances, in: A. Bejan, A.D. Kraus (Eds.), Heat Transfer Handbook, Wiley, Hoboken, New Jersey, 2003, pp. 261–394.
[13] R. Prasher, Thermal interface materials: historical perspective, status, and future directions, Proc. IEEE 94 (8) (2006) 1571–1586.
[14] F. Sarvar, D.C. Whalley, P.P. Conway, Thermal interface materials-A review of the state of the art, in: Electronics Systemintegration Technology Conference, 2006, 1st, IEEE, Dresden, Germany, 2006, pp. 1292–1302.
[15] A.J. McNamara, Y.K. Joshi, Z.M. Zhang, Characterization of nanostructured thermal interface materials-A review. TMNN-2010. Proceedings of the International Symposium on Thermal and Materials Nanoscience and Nanotechnology, Begel House Inc., 2011.
[16] Y. Fu, J. Hansson, Y. Liu, S. Chen, A. Zehri, M.K. Samani, N. Wang, Y. Ni, Y. Zhang, Z.-B. Zhang, Graphene related materials for thermal management, 2D Mater. 7 (1) (2019), 012001.
[17] K.M.F. Shahil, A.A. Balandin, Graphene–Multilayer graphene nanocomposites as highly efficient thermal interface materials, Nano Lett. 12 (2) (2012) 861–867.
[18] D.B. Marchetto, D.C. Moreira, G. Ribatski, A Review on Polymer Heat Sinks for Electronics Cooling Applications, in: 17th Brazilian Congress of Thermal Sciences and Engineering, Águas de Lindóia, SP, Brazil, 2018.
[19] R. Githens, Flexible-tube heat exchangers, Chem. Eng. Prog. 61 (1965) 55–62.
[20] D.R. Anderson, Thermal conductivity of polymers, Chem. Rev. 66 (1966) 677–690.
[21] A. Henry, Thermal transport in polymers, Annual Review of Heat Transfer 17 (2014).
[22] X. Xu, J. Zhou, J. Chen, Thermal transport in conductive polymer–based materials, Adv. Funct. Mater. 30 (2019), 1904704.
[23] C.L. Choy, Thermal conductivity of polymers, Polymer 18 (10) (1977) 984–1004.
[24] P. Dashora, G. Gupta, On the temperature dependence of the thermal conductivity of linear amorphous polymers, Polymer 37 (2) (1996) 231–234.
[25] J.M. Caruthers, K.C. Chao, V. Venkatasubramanian, R. Sy-Siong-Kiao, C.R. Novenario, A. Sundaram, Handbook of Diffusion and Thermal Properties of Polymers and Polymer Solutions, American Institute of Chemical Engineers: New York.
[26] T. Zhang, J. Xu, T. Luo, Extremely High Thermal Conductivity of Aligned Polyacetylene, arXiv:2009.13708.
[27] A. Henry, G. Chen, High thermal conductivity of single polyethylene chains using molecular dynamics simulations, Phys. Rev. Lett. 101 (23) (2008).
[28] E. Fermi, J. Pasta, S. Ulam, Studies of Nonlinear Problems, Report No. LA-1940, Los Alamos Scientific Lab., N. Mex., United States, 1955, 1955.
[29] L.H. Sperling, Introduction to Physical Polymer Science, John Wiley & Sons, Inc., Lehigh University Bethlehem, Pennsylvania, 2006.
[30] A.A. Balandin, Thermal properties of graphene and nanostructured carbon materials, Nat. Mater. 10 (8) (2011) 569–581.
[31] Y. Xu, D. Kraemer, B. Song, Z. Jiang, J. Zhou, J. Loomis, J. Wang, M. Li, H. Ghasemi, X. Huang, X. Li, G. Chen, Nanostructured polymer films with metal-like thermal conductivity, Nat. Commun. 10 (1) (2019) 1771.
[32] X. Xu, J. Chen, J. Zhou, B. Li, Thermal conductivity of polymers and their nanocomposites, Adv. Mater. 30 (17) (2018), 1705544.
[33] X. Xu, J. Zhou, J. Chen, Thermal transport in conductive polymer–based materials, Adv. Funct. Mater. 30 (8) (2020), 1904704.
[34] D. Anderson, Thermal conductivity of polymers, Chem. Rev. 66 (6) (1966) 677–690.
[35] N. Shulumba, O. Hellman, A.J. Minnich, Lattice thermal conductivity of polyethylene molecular crystals from first-principles including nuclear quantum effects, Phys. Rev. Lett. 119 (18) (2017), 185901.
[36] H.S. Calslaw, J.C. Jaeger, Conduction of Heat in Solids, Oxford Science Publications, 1947.
[37] G. Chen, Nanoscale Energy Transport and Conversion, a Parallel Treatment of Electrons, Molecules, Phonons, and Photons, Oxford University Press, 2005.
[38] H. Fujishiro, M. Ikebe, T. Kashima, A. Yamanaka, Thermal conductivity and diffusivity of high-strength polymer fibers, Jpn. J. Appl. Phys. 36 (1, No. 9A) (1997) 5633–5637.
[39] T. Zhang, T. Luo, Morphology-influenced thermal conductivity of polyethylene single chains and crystalline fibers, J. Appl. Phys. 112 (9) (2012), 094304.
[40] J. Liu, R. Yang, Length-dependent thermal conductivity of single extended polymer chains, Phys. Rev. B 86 (10) (2012).
[41] T. Zhang, T. Luo, High-contrast, reversible thermal conductivity regulation utilizing the phase transition of polyethylene nanofibers, ACS Nano 7 (9) (2013) 7592–7600.
[42] X. Wang, M. Kaviany, B. Huang, Phonon coupling and transport in individual polyethylene chains: a comparison study with the bulk crystal, Nanoscale 9 (45) (2017) 18022–18031.
[43] Y. Xu, X. Wang, J. Zhou, B. Song, Z. Jiang, E.M.Y. Lee, S. Huberman, K. K. Gleason, G. Chen, Molecular engineered conjugated polymer with high thermal conductivity, Science Advances 4 (3) (2018) eaar3031.
[44] H.W. Hill, D.G. Brady, Properties, environmental stability, and molding characteristics of polyphenylene sulfide, Polym. Eng. Sci. 16 (12) (1976) 831–835.
[45] B. Poulaert, J.-C. Chielens, C. Vandenhende, J.-P. Issi, R. Legras, Thermal conductivity of highly oriented polyethylene fibres, Polym. Commun. 31 (4) (1990) 148–151.
[46] H.-C. Chien, W.-T. Peng, T.-H. Chiu, P.-H. Wu, Y.-J. Liu, C.-W. Tu, C.-L. Wang, M.-C. Lu, Heat transfer of semicrystalline nylon nanofibers, ACS Nano 14 (3) (2020) 2939–2946.
[47] R. Muthaiah, J. Garg, Temperature effects in the thermal conductivity of aligned amorphous polyethylene—a molecular dynamics study, J. Appl. Phys. 124 (10) (2018), 105102.
[48] V. Singh, T.L. Bougher, A. Weathers, Y. Cai, K. Bi, M.T. Pettes, S.A. McMenamin, W. Lv, D.P. Resler, T.R. Gattuso, High thermal conductivity of chain-oriented amorphous polythiophene, Nat. Nanotechnol. 9 (5) (2014) 384–390.
[49] H. Fujishiro, M. Ikebe, T. Kashima, A. Yamanaka, Drawing effect on thermal properties of high-strength polyethylene fibers, Jpn. J. Appl. Phys. 37 (4R) (1998) 1994.
[50] C. Choy, Y. Wong, G. Yang, T. Kanamoto, Elastic modulus and thermal conductivity of ultradrawn polyethylene, J. Polym. Sci. B Polym. Phys. 37 (23) (1999) 3359–3367.
[51] R. Shrestha, P. Li, B. Chatterjee, T. Zheng, X. Wu, Z. Liu, T. Luo, S. Choi, K. Hippalgaonkar, M.P. de Boer, S. Shen, Crystalline polymer nanofibers with ultra-high strength and thermal conductivity, Nat. Commun. 9 (1) (2018).
[52] S. Shen, A. Henry, J. Tong, R. Zheng, G. Chen, Polyethylene nanofibres with very high thermal conductivities, Nat. Nanotechnol. 5 (4) (2010) 251–255.
[53] X. Wang, V. Ho, R.A. Segalman, D.G. Cahill, Thermal conductivity of high-modulus polymer fibers, Macromolecules 46 (12) (2013) 4937–4943.
[54] K. Utimula, T. Ichibha, R. Maezono, K. Hongo, Ab initio search of polymer crystals with high thermal conductivity, Chem. Mater. 31 (13) (2019) 4649–4656.
[55] C.L. Choy, Y. Fei, T.G. Xi, Thermal conductivity of gel-spun polyethylene fibers, J. Polym. Sci. B Polym. Phys. 31 (3) (1993) 365–370.
[56] D.E. Kline, Thermal conductivity studies of polymers, J. Polym. Sci. 50 (154) (1961) 441–450.
[57] T. Zhang, X. Wu, T. Luo, Polymer nanofibers with outstanding thermal conductivity and thermal stability: fundamental linkage between molecular characteristics and macroscopic thermal properties, J. Phys. Chem. C 118 (36) (2014) 21148–21159.
[58] H. Chen, V.V. Ginzburg, J. Yang, Y. Yang, W. Liu, Y. Huang, L. Du, B. Chen, Thermal conductivity of polymer-based composites: fundamentals and applications, Prog. Polym. Sci. 59 (2016) 41–85.
[59] J. Yu, B. Sundqvist, B. Tonpheng, O. Andersson, Thermal conductivity of highly crystallized polyethylene, Polymer 55 (1) (2014) 195–200.
[60] A.J. de Vries, C. Bonnebat, J. Beautemps, Uni- and biaxial orientation of polymer films and sheets, J. Polym. Sci., Polym. Symp. 58 (1) (1977) 109–156.
[61] T. Kanamoto, A. Tsuruta, K. Tanaka, M. Takeda, R.S. Porter, Super-drawing of ultrahigh molecular weight polyethylene. 1. Effect of techniques on drawing of single crystal mats, Macromolecules 21 (2) (1988) 470–477.
[62] P.A. Irvine, P. Smith, Development of the axial Young's modulus with draw ratio of flexible-chain polymers, Macromolecules 19 (1) (1986) 240–242.
[63] G.S.Y. Yeh, P.H. Geil, Strain-induced crystallization of polyethylene terephthalate, J. Macromol. Sci., Part B 1 (1967) 251–277.
[64] I.J. Rao, K.R. Rajagopal, A study of strain-induced crystallization of polymers, Int. J. Solid Struct. 38 (6-7) (2001) 1149–1167.
[65] E. Forestier, C. Combeaud, N. Guigo, N. Sbirrazzuoli, N. Billon, Understanding of strain-induced crystallization developments scenarios for polyesters: comparison of poly(ethylene furanoate), PEF, and poly(ethylene terephthalate), PET, Polymer 203 (2020), 122755.
[66] C.L. Choy, Y.W. Wong, G.W. Yang, T. Kanamoto, Elastic modulus and thermal conductivity of ultradrawn polyethylene, J. Polym. Sci. B Polym. Phys. 37 (23) (1999) 3359–3367.
[67] V.M. Litvinov, J. Xu, C. Melian, D.E. Demco, M. Möller, J. Simmelink, Morphology, chain dynamics, and domain sizes in highly drawn gel-spun ultrahigh molecular weight polyethylene fibers at the final stages of drawing by SAXS, WAXS, and solid-state NMR, Macromolecules 44 (23) (2011) 9254–9266.
[68] A.G. Gibson, D. Greig, M. Sahota, I.M. Ward, C.L. Choy, Thermal conductivity of ultrahigh-modulus polyethylene, J. Polym. Sci., Polym. Lett. Ed. 15 (1977) 183–192.
[69] S. Ronca, T. Igarashi, G. Forte, S. Rastogi, Metallic-like thermal conductivity in a lightweight insulator: solid-state processed ultra high molecular weight polyethylene tapes and films, Polymer 123 (2017) 203–210.
[70] C.L. Choy, W.H. Luk, F.C. Chen, Thermal conductivity of highly oriented polyethylene, Polymer 19 (2) (1978) 155–162.
[71] D.B. Mergenthaler, M. Pietralla, S. Roy, H.G. Kilian, Thermal conductivity in ultraoriented polyethylene, Macromolecules 25 (13) (1992) 3500–3502.

[72] J. Hennig, W. Knappe, Anisotropy of thermal conductivity in stretched amorphous linear polymers and in strained elastomers, J. Polym. Sci. Part C: Polymer Symposia 6 (1) (2007) 167–174.
[73] K. Eiermann, Thermal conductivity of high polymers, J. Polym. Sci. Part C: Polymer Symposia 6 (1) (2007) 157–165.
[74] D.N. Simavilla, J.D. Schieber, D.C. Venerus, Anisotropic thermal transport in a crosslinked polyisoprene rubber subjected to uniaxial elongation, J. Polym. Sci. B Polym. Phys. 50 (23) (2012) 1638–1644.
[75] A.B. Robbins, S.X. Drakopoulos, I. Martin-Fabiani, S. Ronca, A.J. Minnich, Ballistic thermal phonons traversing nanocrystalline domains in oriented polyethylene, Proc. Natl. Acad. Sci. Unit. States Am. 116 (35) (2019) 17163–17168.
[76] J. Hennig, Anisotropy and structure in uniaxially stretched amorphous high polymers: amorphous high polymers, J. Polym. Sci. Part C: Polymer Symposia 16 (5) (1967) 2751–2761.
[77] S.T.J. Peng, R.F. Landel, Induced anisotropy of thermal conductivity of polymer solids under large strains, J. Appl. Polym. Sci. 19 (1) (1975) 49–68.
[78] J.E. Huheey, E.A. Keiter, R.L. Keiter, Inorganic Chemistry : Principles of Structure and Reactivity, HarperCollins College Publishers, New York, NY, 1993.
[79] X. Liu, The controlled evolution of a polymer single crystal, Science 307 (5716) (2005) 1763–1766.
[80] D.J. Hitt, M. Gilbert, A machine for the biaxial stretching of polymers, Polym. Test. 13 (3) (1994) 219–237.
[81] I. Greenfeld, X. Sui, H.D. Wagner, Stiffness, strength, and toughness of electrospun nanofibers: effect of flow-induced molecular orientation, Macromolecules 49 (17) (2016) 6518–6530.
[82] J. Xue, T. Wu, Y. Dai, Y. Xia, Electrospinning and electrospun nanofibers: methods, materials, and applications, Chem. Rev. 119 (8) (2019) 5298–5415.
[83] J. Ma, Q. Zhang, A. Mayo, Z. Ni, H. Yi, Y. Chen, R. Mu, L.M. Bellan, D. Li, Thermal conductivity of electrospun polyethylene nanofibers, Nanoscale 7 (40) (2015) 16899–16908.
[84] Z. Zhong, M.C. Wingert, J. Strzalka, H.-H. Wang, T. Sun, J. Wang, R. Chen, Z. Jiang, Structure-induced enhancement of thermal conductivities in electrospun polymer nanofibers, Nanoscale 6 (14) (2014) 8283–8291.
[85] C. Lu, S.W. Chiang, H. Du, J. Li, L. Gan, X. Zhang, X. Chu, Y. Yao, B. Li, F. Kang, Thermal conductivity of electrospinning chain-aligned polyethylene oxide (PEO), Polymer 115 (2017) 52–59.
[86] Y. Zhang, X. Zhang, L. Yang, Q. Zhang, M.L. Fitzgerald, A. Ueda, Y. Chen, R. Mu, D. Li, L.M. Bellan, Thermal transport in electrospun vinyl polymer nanofibers: effects of molecular weight and side groups, Soft Matter 14 (47) (2018) 9534–9541.
[87] C. Canetta, S. Guo, A. Narayanaswamy, Measuring thermal conductivity of polystyrene nanowires using the dual-cantilever technique, Rev. Sci. Instrum. 85 (10) (2014), 104901.
[88] J.V. Goicochea, T. Brunschwiler, J. Zurcher, H. Wolf, K. Matsumoto, B. Michel, Enhanced centrifugal percolating thermal underfills based on neck formation by capillary bridging, in: Thermal and Thermomechanical Phenomena in Electronic Systems (ITherm), 2012 13th IEEE Intersociety Conference on, IEEE, San Diego, 2012, pp. 1234–1241.
[89] H. Li, K.I. Jacob, C.P. Wong, An improvement of thermal conductivity of underfill materials for flip-chip packages, IEEE Trans. Adv. Packag. 26 (1) (2003) 25–32.
[90] J. Zuercher, J. Goicochea, K. Matsumoto, B. Michel, T. Brunschwiler, Centrifugal formulation of percolating thermal underfills for flip-chip applications, in: 2012 7th International Conference on Integrated Power Electronics Systems (CIPS), IEEE, Nuremberg, 2012, pp. 1–6.
[91] Z. Lin, L. Yan, M. Kyoung-sik, W. Ching-Ping, Enhanced thermal transport of hexagonal boron nitride filled polymer composite by magnetic field-assisted alignment, in: 2013 IEEE 63rd Electronic Components and Technology Conference (ECTC), IEEE, Las Vegas, 2013, pp. 1692–1696.
[92] K. Suzuki, O. Suzuki, K. Muramatu, T. Yuda, K. Isobe, H. Maruyama, H. Fukuyama, High thermally conductive underfill for flip-chip applications, in: 2001. Proceedings. International Symposium on Advanced Packaging Materials: Processes, Properties and Interfaces, IEEE, Braselton, 2001, pp. 46–50.
[93] Q. Liang, M. Kyoung-sik, J. Hongjin, C.C. Wong, Thermal conductivity enhancement of epoxy composites by interfacial covalent bonding for underfill and thermal interfacial materials in Cu/low-K application, IEEE Trans. Compon. Packag. Manuf. Technol. 2 (10) (2012) 1571–1579.
[94] K.M.F. Shahil, A.A. Balandin, Graphene-multilayer graphene nanocomposites as highly efficient thermal interface materials, Nano Lett. 12 (2) (2012) 861–867.
[95] M.J. Biercuk, M.C. Llaguno, M. Radosavljevic, J.K. Hyun, A.T. Johnson, J. E. Fischer, Carbon nanotube composites for thermal management, Appl. Phys. Lett. 80 (15) (2002) 2767–2769.
[96] Z. Lin, Y. Yagang, A. McNamara, M. Kyoung-sik, C.P. Wong, Single/few-layer boron nitride-based nanocomposites for high thermal conductivity underfills, in: 2012 IEEE 62nd Electronic Components and Technology Conference (ECTC), IEEE, San Diego, 2012, pp. 1437–1441.
[97] S.N. Leung, Thermally conductive polymer composites and nanocomposites: processing-structure-property relationships, Compos. B Eng. 150 (2018) 78–92.
[98] Y. Guo, K. Ruan, X. Yang, T. Ma, J. Kong, N. Wu, J. Zhang, J. Gu, Z. Guo, Constructing fully carbon-based fillers with a hierarchical structure to fabricate highly thermally conductive polyimide nanocomposites, J. Mater. Chem. C 7 (23) (2019) 7035–7044.
[99] X. Huang, J. Pingkai, T. Tanaka, A review of dielectric polymer composites with high thermal conductivity, Electrical Insulation Magazine, IEEE 27 (4) (2011) 8–16.
[100] H. Ishida, S. Rimdusit, Very high thermal conductivity obtained by boron nitride-®lled polybenzoxazine, Thermochim. Acta 320 (1998) 10.
[101] W.L. Ong, S.M. Rupich, D.V. Talapin, A.J.H. McGaughey, J.A. Malen, Surface chemistry mediates thermal transport in three-dimensional nanocrystal arrays, Nat. Mater. 12 (5) (2013) 410–415.
[102] M. Liu, Y. Ma, R.Y. Wang, Modifying thermal transport in colloidal nanocrystal solids with surface chemistry, ACS Nano 9 (12) (2015) 12079–12087.
[103] A. Minnich, G. Chen, Modified effective medium formulation for the thermal conductivity of nanocomposites, Appl. Phys. Lett. 91 (7) (2007), 073105.
[104] J. Wang, J.K. Carson, M.F. North, D.J. Cleland, A new approach to modelling the effective thermal conductivity of heterogeneous materials, Int. J. Heat Mass Tran. 49 (17) (2006) 3075–3083.
[105] C.-W. Nan, R. Birringer, D.R. Clarke, H. Gleiter, Effective thermal conductivity of particulate composites with interfacial thermal resistance, J. Appl. Phys. 81 (10) (1997) 6692–6699.
[106] D. Hasselman, L.F. Johnson, Effective thermal conductivity of composites with interfacial thermal barrier resistance, J. Compos. Mater. 21 (6) (1987) 508–515.
[107] Y. Benveniste, Effective thermal conductivity of composites with a thermal contact resistance between the constituents: nondilute case, J. Appl. Phys. 61 (8) (1987) 2840–2843.
[108] X.-Q. Wang, A.S. Mujumdar, Heat transfer characteristics of nanofluids: a review, Int. J. Therm. Sci. 46 (1) (2007) 1–19.
[109] Q. Hao, H. Zhao, Y. Xiao, D. Xu, Thermal investigation of nanostructured bulk thermoelectric materials with hierarchical structures: an effective medium approach, J. Appl. Phys. 123 (1) (2018), 014303.
[110] A. Minnich, G. Chen, Modified effective medium formulation for the thermal conductivity of nanocomposites, Appl. Phys. Lett. 91 (7) (2007), 073105.
[111] G. Wei, Y. Liu, X. Zhang, F. Yu, X. Du, Thermal conductivities study on silica aerogel and its composite insulation materials, Int. J. Heat Mass Tran. 54 (11) (2011) 2355–2366.
[112] S.O. Zeng, A. Hunt, R. Greif, Geometric structure and thermal conductivity of porous medium silica aerogel, J. Heat Tran. 117 (1995) 1055–1058.
[113] X. Wu, B.L. Greenberg, Y. Zhang, J.T. Held, D. Huang, J.G. Barriocanal, K. A. Mkhoyan, E.S. Aydil, U. Kortshagen, X. Wang, Thermal transport in ZnO nanocrystal networks synthesized by nonthermal plasma, Physical Review Materials 4 (8) (2020), 086001.
[114] M. Levin, M. Miller, Maxwell a treatise on electricity and magnetism, Usp. Fiz. Nauk 135 (3) (1981) 425–440.
[115] A. Eucken, Thermal conductivity of ceramic refractory materials: calculation from thermal conductivity of constituents, Ceramic Abstr 11 (1932) 576.
[116] Q. Hao, Y. Xiao, H. Zhao, Analytical model for phonon transport analysis of periodic bulk nanoporous structures, Appl. Therm. Eng. 111 (2017) 1409–1416.
[117] Y. Xiao, Q. Chen, D. Ma, N. Yang, Q. Hao, Phonon transport within periodic porous structures - from classical phonon size effects to wave effects, ES Materials & Manufacturing 5 (2019) 2–18.
[118] A.G. Every, Y. Tzou, D. Hasselman, R. Raj, The effect of particle size on the thermal conductivity of ZnS/diamond composites, Acta Metall. Mater. 40 (1) (1992) 123–129.
[119] R.S. Prasher, X.J. Hu, Y. Chalopin, N. Mingo, K. Lofgreen, S. Volz, F. Cleri, P. Keblinski, Turning carbon nanotubes from exceptional heat conductors into insulators, Phys. Rev. Lett. 102 (10) (2009) 105901.
[120] L. Hu, T. Desai, P. Keblinski, Thermal transport in graphene-based nanocomposite, J. Appl. Phys. 110 (3) (2011), 033517.
[121] M. Bhattacharya, Polymer nanocomposites—a comparison between carbon nanotubes, graphene, and clay as nanofillers, Materials 9 (4) (2016) 262.
[122] R.S. Prasher, J. Shipley, S. Prstic, P. Koning, J.-l. Wang, Thermal resistance of particle laden polymeric thermal interface materials, in: ASME International Mechanical Engineering Congress and Exposition, 2003, pp. 431–439.
[123] C. Huang, X. Qian, R. Yang, Thermal conductivity of polymers and polymer nanocomposites, Mater. Sci. Eng. R Rep. 132 (2018) 1–22.
[124] S.T. Huxtable, D.G. Cahill, S. Shenogin, P. Keblinski, Relaxation of vibrational energy in fullerene suspensions, Chem. Phys. Lett. 407 (1) (2005) 129–134.
[125] F. Gong, K. Bui, D.V. Papavassiliou, H.M. Duong, Thermal transport phenomena and limitations in heterogeneous polymer composites containing carbon nanotubes and inorganic nanoparticles, Carbon 78 (2014) 305–316.
[126] L. Zhang, L. Liu, Polymeric self-assembled monolayers anomalously improve thermal transport across graphene/polymer interfaces, ACS Appl. Mater. Interfaces 9 (34) (2017) 28949–28958.
[127] S. Shenogin, L. Xue, R. Ozisik, P. Keblinski, D.G. Cahill, Role of thermal boundary resistance on the heat flow in carbon-nanotube composites, J. Appl. Phys. 95 (12) (2004) 8136–8144.
[128] E.T. Swartz, R.O. Pohl, Thermal boundary resistance, Rev. Mod. Phys. 61 (3) (1989) 605–668.
[129] K. Ruan, X. Shi, Y. Guo, J. Gu, Interfacial thermal resistance in thermally conductive polymer composites: a review, Composites Communications (2020), 100518.
[130] J. Ma, C. Nan, Effective-medium approach to thermal conductivity of heterogeneous materials, Annual Review of Heat Transfer 17 (2014).
[131] C.-W. Nan, Physics of inhomogeneous inorganic materials, Prog. Mater. Sci. 37 (1) (1993) 1–116.
[132] C.-W. Nan, G. Liu, Y. Lin, M. Li, Interface effect on thermal conductivity of carbon nanotube composites, Appl. Phys. Lett. 85 (16) (2004) 3549–3551.
[133] M.B. Bryning, D.E. Milkie, M.F. Islam, J.M. Kikkawa, A.G. Yodh, Thermal conductivity and interfacial resistance in single-wall carbon nanotube epoxy composites, Appl. Phys. Lett. 87 (16) (2005), 161909.

[134] S. Chen, A.L. Moore, W. Cai, J.W. Suk, J. An, C. Mishra, C. Amos, C.W. Magnuson, J. Kang, L. Shi, Raman measurements of thermal transport in suspended monolayer graphene of variable sizes in vacuum and gaseous environments, ACS Nano 5 (1) (2011) 321–328.
[135] S. Chen, Q. Wu, C. Mishra, J. Kang, H. Zhang, K. Cho, W. Cai, A.A. Balandin, R. S. Ruoff, Thermal conductivity of isotopically modified graphene, Nat. Mater. 11 (3) (2012) 203–207.
[136] Q. Jiang, X. Wang, Y. Zhu, D. Hui, Y. Qiu, Mechanical, electrical and thermal properties of aligned carbon nanotube/polyimide composites, Compos. B Eng. 56 (2014) 408–412.
[137] A.M. Marconnet, N. Yamamoto, M.A. Panzer, B.L. Wardle, K.E. Goodson, Thermal conduction in aligned carbon nanotube–polymer nanocomposites with high packing density, ACS Nano 5 (6) (2011) 4818–4825.
[138] H. Huang, C.H. Liu, Y. Wu, S. Fan, Aligned carbon nanotube composite films for thermal management, Adv. Mater. 17 (13) (2005) 1652–1656.
[139] E. Choi, J. Brooks, D. Eaton, M. Al-Haik, M. Hussaini, H. Garmestani, D. Li, K. Dahmen, Enhancement of thermal and electrical properties of carbon nanotube polymer composites by magnetic field processing, J. Appl. Phys. 94 (9) (2003) 6034–6039.
[140] Y.-F. Zhang, D. Han, Y.-H. Zhao, S.-L. Bai, High-performance thermal interface materials consisting of vertically aligned graphene film and polymer, Carbon 109 (2016) 552–557.
[141] P. Bonnet, D. Sireude, B. Garnier, O. Chauvet, Thermal properties and percolation in carbon nanotube-polymer composites, Appl. Phys. Lett. 91 (20) (2007), 201910.
[142] S. Kumar, M. Alam, J. Murthy, Effect of percolation on thermal transport in nanotube composites, Appl. Phys. Lett. 90 (10) (2007), 104105.
[143] R. Zheng, J. Gao, J. Wang, S.-P. Feng, H. Ohtani, J. Wang, G. Chen, Thermal percolation in stable graphite suspensions, Nano Lett. 12 (1) (2012) 188–192.
[144] F. Kargar, Z. Barani, R. Salgado, B. Debnath, J.S. Lewis, E. Aytan, R.K. Lake, A. A. Balandin, Thermal percolation threshold and thermal properties of composites with high loading of graphene and boron nitride fillers, ACS Appl. Mater. Interfaces 10 (43) (2018) 37555–37565.
[145] S.T. Huxtable, D.G. Cahill, S. Shenogin, L. Xue, R. Ozisik, P. Barone, M. Usrey, M. S. Strano, G. Siddons, M. Shim, Interfacial heat flow in carbon nanotube suspensions, Nat. Mater. 2 (11) (2003) 731–734.
[146] L.E. Nielsen, Thermal conductivity of particulate-filled polymers, J. Appl. Polym. Sci. 17 (12) (1973) 3819–3820.
[147] L.E. Nielsen, The thermal and electrical conductivity of two-phase systems, Ind. Eng. Chem. Fund. 13 (1) (1974) 17–20.
[148] K. Kong, M. Mariatti, A. Rashid, J. Busfield, Enhanced conductivity behavior of polydimethylsiloxane (PDMS) hybrid composites containing exfoliated graphite nanoplatelets and carbon nanotubes, Compos. B Eng. 58 (2014) 457–462.
[149] S.-Y. Yang, W.-N. Lin, Y.-L. Huang, H.-W. Tien, J.-Y. Wang, C.-C.M. Ma, S.-M. Li, Y.-S. Wang, Synergetic effects of graphene platelets and carbon nanotubes on the mechanical and thermal properties of epoxy composites, Carbon 49 (3) (2011) 793–803.
[150] S. Paszkiewicz, A. Szymczyk, R. Pilawka, B. Przybyszewski, A. Czulak, Z. RosŁaniec, Improved thermal conductivity of poly (trimethylene terephthalate-block-poly (tetramethylene oxide) based nanocomposites containing hybrid single-walled carbon nanotubes/graphene nanoplatelets fillers, Adv. Polym. Technol. 36 (2) (2017) 236–242.
[151] F. Zhang, Q. Li, Y. Liu, S. Zhang, C. Wu, W. Guo, Improved thermal conductivity of polycarbonate composites filled with hybrid exfoliated graphite/multi-walled carbon nanotube fillers, J. Therm. Anal. Calorim. 123 (1) (2016) 431–437.
[152] A. Yu, P. Ramesh, X. Sun, E. Bekyarova, M.E. Itkis, R.C. Haddon, Enhanced thermal conductivity in a hybrid graphite nanoplatelet–carbon nanotube filler for epoxy composites, Adv. Mater. 20 (24) (2008) 4740–4744.
[153] J.-P. Cao, J. Zhao, X. Zhao, F. You, H. Yu, G.-H. Hu, Z.-M. Dang, High thermal conductivity and high electrical resistivity of poly (vinylidene fluoride)/ polystyrene blends by controlling the localization of hybrid fillers, Compos. Sci. Technol. 89 (2013) 142–148.
[154] Z. Li, D. Ju, L. Han, L. Dong, Formation of more efficient thermally conductive pathways due to the synergistic effect of boron nitride and alumina in poly (3-hydroxylbutyrate), Thermochim. Acta 652 (2017) 9–16.
[155] G. He, X. Zhou, J. Liu, J. Zhang, L. Pan, S. Liu, Synergetic enhancement of thermal conductivity for highly explosive-filled polymer composites through hybrid carbon nanomaterials, Polym. Compos. 39 (S3) (2018) E1452–E1462.
[156] K. Wu, C. Lei, R. Huang, W. Yang, S. Chai, C. Geng, F. Chen, Q. Fu, Design and preparation of a unique segregated double network with excellent thermal conductive property, ACS Appl. Mater. Interfaces 9 (8) (2017) 7637–7647.
[157] X. Huang, C. Zhi, P. Jiang, Toward effective synergetic effects from graphene nanoplatelets and carbon nanotubes on thermal conductivity of ultrahigh volume fraction nanocarbon epoxy composites, J. Phys. Chem. C 116 (44) (2012) 23812–23820.
[158] M.T. Pettes, H. Ji, R.S. Ruoff, L. Shi, Thermal transport in three-dimensional foam architectures of few-layer graphene and ultrathin graphite, Nano Lett. 12 (6) (2012) 2959–2964.
[159] L.-l. Liu, J. Fan, P.-p. Chen, J. Du, F.-l. Yang, Synthesis of heat exchanger networks considering fouling, aging, and cleaning, Ind. Eng. Chem. Res. 54 (1) (2015) 296–306.
[160] J. Klett, R. Hardy, E. Romine, C. Walls, T. Burchell, High-thermal-conductivity, mesophase-pitch-derived carbon foams: effect of precursor on structure and properties, Carbon 38 (7) (2000) 953–973.
[161] R. Sengupta, M. Bhattacharya, S. Bandyopadhyay, A.K. Bhowmick, A review on the mechanical and electrical properties of graphite and modified graphite reinforced polymer composites, Prog. Polym. Sci. 36 (5) (2011) 638–670.
[162] Y.C. Li, G.H. Chen, HDPE/expanded graphite nanocomposites prepared via masterbatch process, Polym. Eng. Sci. 47 (6) (2007) 882–888.
[163] J. Wang, W. Chow, A brief review on fire retardants for polymeric foams, J. Appl. Polym. Sci. 97 (1) (2005) 366–376.
[164] W. Feng, M. Qin, P. Lv, J. Li, Y. Feng, A three-dimensional nanostructure of graphite intercalated by carbon nanotubes with high cross-plane thermal conductivity and bending strength, Carbon 77 (2014) 1054–1064.
[165] S. Zhou, L. Yu, X. Song, J. Chang, H. Zou, M. Liang, Preparation of highly thermally conducting polyamide 6/graphite composites via low-temperature in situ expansion, J. Appl. Polym. Sci. 131 (1) (2014).
[166] S. Kim, M. Poostforush, J. Kim, S. Lee, Thermal diffusivity of in-situ exfoliated graphite intercalated compound/polyamide and graphite/polyamide composites, Express Polym. Lett. 6 (6) (2012).
[167] A. Yu, P. Ramesh, M.E. Itkis, E. Bekyarova, R.C. Haddon, Graphite nanoplatelet–epoxy composite thermal interface materials, J. Phys. Chem. C 111 (21) (2007) 7565–7569.
[168] S. Ganguli, A.K. Roy, D.P. Anderson, Improved thermal conductivity for chemically functionalized exfoliated graphite/epoxy composites, Carbon 46 (5) (2008) 806–817.
[169] C.-C. Teng, C.-C.M. Ma, C.-H. Lu, S.-Y. Yang, S.-H. Lee, M.-C. Hsiao, M.-Y. Yen, K.-C. Chiou, T.-M. Lee, Thermal conductivity and structure of non-covalent functionalized graphene/epoxy composites, Carbon 49 (15) (2011) 5107–5116.
[170] K.M. Shahil, A.A. Balandin, Graphene–multilayer graphene nanocomposites as highly efficient thermal interface materials, Nano Lett. 12 (2) (2012) 861–867.
[171] S.H. Song, K.H. Park, B.H. Kim, Y.W. Choi, G.H. Jun, D.J. Lee, B.S. Kong, K. W. Paik, S. Jeon, Enhanced thermal conductivity of epoxy–graphene composites by using non-oxidized graphene flakes with non-covalent functionalization, Adv. Mater. 25 (5) (2013) 732–737.
[172] H. Jung, S. Yu, N.-S. Bae, S.M. Cho, R.H. Kim, S.H. Cho, I. Hwang, B. Jeong, J. S. Ryu, J. Hwang, High through-plane thermal conduction of graphene nanoflake filled polymer composites melt-processed in an L-shape kinked tube, ACS Appl. Mater. Interfaces 7 (28) (2015) 15256–15262.
[173] M. Shtein, R. Nadiv, M. Buzaglo, K. Kahil, O. Regev, Thermally conductive graphene-polymer composites: size, percolation, and synergy effects, Chem. Mater. 27 (6) (2015) 2100–2106.
[174] I. Kholmanov, J. Kim, E. Ou, R.S. Ruoff, L. Shi, Continuous carbon nanotube–ultrathin graphite hybrid foams for increased thermal conductivity and suppressed subcooling in composite phase change materials, ACS Nano 9 (12) (2015) 11699–11707.
[175] D. Suh, C.M. Moon, D. Kim, S. Baik, Ultrahigh thermal conductivity of interface materials by silver-functionalized carbon nanotube phonon conduits, Adv. Mater. 28 (33) (2016) 7220–7227.
[176] H.S. Kim, H.S. Bae, J. Yu, S.Y. Kim, Thermal conductivity of polymer composites with the geometrical characteristics of graphene nanoplatelets, Sci. Rep. 6 (1) (2016) 1–9.
[177] X. Shen, Z. Wang, Y. Wu, X. Liu, Y.-B. He, J.-K. Kim, Multilayer graphene enables higher efficiency in improving thermal conductivities of graphene/epoxy composites, Nano Lett. 16 (6) (2016) 3585–3593.
[178] H.S. Kim, J.H. Kim, W.Y. Kim, H.S. Lee, S.Y. Kim, M.-S. Khil, Volume control of expanded graphite based on inductively coupled plasma and enhanced thermal conductivity of epoxy composite by formation of the filler network, Carbon 119 (2017) 40–46.
[179] J.-u. Jang, H.C. Park, H.S. Lee, M.-S. Khil, S.Y. Kim, Electrically and thermally conductive carbon fibre fabric reinforced polymer composites based on nanocarbons and an in-situ polymerizable cyclic oligoester, Sci. Rep. 8 (1) (2018) 1–9.
[180] J. Chen, B. Liu, L. Yan, Nanoscale thermal transport in epoxy matrix composite materials reinforced with carbon nanotubes and graphene nanoplatelets, J. Nano Res. 21 (11) (2019) 256.
[181] J. Chen, X. Gao, W. Song, Effect of various carbon nanofillers and different filler aspect ratios on the thermal conductivity of epoxy matrix nanocomposites, Results Phys 15 (2019), 102771.
[182] J. Huang, J. Park, W. Wang, C.J. Murphy, D.G. Cahill, Ultrafast thermal analysis of surface functionalized gold nanorods in aqueous solution, ACS Nano 7 (1) (2012) 589–597.
[183] J. Park, J. Huang, W. Wang, C.J. Murphy, D.G. Cahill, Heat transport between Au nanorods, surrounding liquids, and solid supports, J. Phys. Chem. C 116 (50) (2012) 26335–26341.
[184] X. Wu, Y. Ni, J. Zhu, N.D. Burrows, C.J. Murphy, T. Dumitrica, X. Wang, Thermal transport across surfactant layers on gold nanorods in aqueous solution, ACS Appl. Mater. Interfaces 8 (16) (2016) 10581–10589.
[185] D. Xu, R. Hanus, Y. Xiao, S. Wang, G.J. Snyder, Q. Hao, Thermal boundary resistance correlated with strain energy in individual Si film-wafer twist boundaries, Materials Today Physics 6 (2018) 53–59.
[186] S. Wang, D. Xu, R. Gurunathan, G.J. Snyder, Q. Hao, Thermal studies of individual Si/Ge heterojunctions — the influence of the alloy layer on the heterojunction, Journal of Materiomics 6 (2) (2020) 248–255.
[187] F.-p. Du, W. Yang, F. Zhang, C.-Y. Tang, S.-p. Liu, L. Yin, W.-C. Law, Enhancing the heat transfer efficiency in graphene–epoxy nanocomposites using a magnesium oxide–graphene hybrid structure, ACS Appl. Mater. Interfaces 7 (26) (2015) 14397–14403.

[188] F. Wang, X. Zeng, Y. Yao, R. Sun, J. Xu, C.-P. Wong, Silver nanoparticle-deposited boron nitride nanosheets as fillers for polymeric composites with high thermal conductivity, Sci. Rep. 6 (1) (2016) 1–9.
[189] L. Zhang, L. Liu, Hierarchically hydrogen-bonded graphene/polymer interfaces with drastically enhanced interfacial thermal conductance, Nanoscale 11 (8) (2019) 3656–3664.
[190] Y. Gao, F. Müller-Plathe, Increasing the thermal conductivity of graphene-polyamide-6, 6 nanocomposites by surface-grafted polymer chains: calculation with molecular dynamics and effective-medium approximation, J. Phys. Chem. B 120 (7) (2016) 1336–1346.
[191] Y. Guo, X. Yang, K. Ruan, J. Kong, M. Dong, J. Zhang, J. Gu, Z. Guo, Reduced graphene oxide heterostructured silver nanoparticles significantly enhanced thermal conductivities in hot-pressed electrospun polyimide nanocomposites, ACS Appl. Mater. Interfaces 11 (28) (2019) 25465–25473.
[192] Y. Guo, Z. Lyu, X. Yang, Y. Lu, K. Ruan, Y. Wu, J. Kong, J. Gu, Enhanced thermal conductivities and decreased thermal resistances of functionalized boron nitride/polyimide composites, Compos. B Eng. 164 (2019) 732–739.
[193] R.S. Prasher, J.C. Matayabas, Thermal contact resistance of cured gel polymeric thermal interface material, IEEE Trans. Compon. Packag. Technol. 27 (4) (2004) 702–709.
[194] T. Zhan, L. Fang, Y. Xu, Prediction of thermal boundary resistance by the machine learning method, Sci. Rep. 7 (1) (2017) 1–9.
[195] Y.-J. Wu, L. Fang, Y. Xu, Predicting interfacial thermal resistance by machine learning, npj Computational Materials 5 (1) (2019) 56.
[196] H. Zhang, K. Hippalgaonkar, T. Buonassisi, O.M. Løvvik, E. Sagvolden, D. Ding, Machine Learning for Novel Thermal-Materials Discovery: Early Successes, Opportunities, and Challenges, 2019 arXiv preprint arXiv:1901.05801.
[197] S.F. Hansen, A. Lennquist, Carbon nanotubes added to the SIN list as a nanomaterial of very high concern, Nat. Nanotechnol. 15 (1) (2020) 3–4.
[198] Y. Lin, Y. Zhang, J. Li, H. Kong, Q. Yan, J. Zhang, W. Li, N. Ren, Y. Cui, T. Zhang, X. Cai, Q. Li, A. Li, J. Shi, L. Wang, Y. Zhu, C. Fan, Blood exposure to graphene oxide may cause anaphylactic death in non-human primates, Nano Today 35 (2020), 100922.
[199] G. Zhang, Y.-W. Zhang, Strain effects on thermoelectric properties of two-dimensional materials, Mech. Mater. 91 (2015) 382–398.
[200] M. Chu, Y. Sun, U. Aghoram, S.E. Thompson, Strain: a solution for higher carrier mobility in nanoscale MOSFETs, Annu. Rev. Mater. Res. 39 (2009) 203–229.
[201] X. Yang, Y. Guo, Y. Han, Y. Li, T. Ma, M. Chen, J. Kong, J. Zhu, J. Gu, Significant improvement of thermal conductivities for BNNS/PVA composite films via electrospinning followed by hot-pressing technology, Compos. B Eng. 175 (2019), 107070.
[202] Y. Han, X. Shi, X. Yang, Y. Guo, J. Zhang, J. Kong, J. Gu, Enhanced thermal conductivities of epoxy nanocomposites via incorporating in-situ fabricated hetero-structured SiC-BNNS fillers, Compos. Sci. Technol. 187 (2020), 107944.